Intramolecular Chalcogen−Nitrogen Interactions: Molecular and Electronic Structures of Geometrical Isomers of the Diazenes RSN═C(R′)N═NC(R′)═NSR

Tristram Chivers,* Ian Krouse, Masood Parvez, Ignacio Vargas-Baca, Tom Ziegler,* and Peter Zoricak

Department of Chemistry, The University of Calgary, Calgary, Alberta, Canada T2N 1N4

Received April 26, 1996[⊗]

The sulfur-containing diazenes ArSN═C(Ar′)N═NC(Ar′)═NSAr (**1d**, Ar = Ar′ = 4-$CH_3C_6H_4$; **3b**, Ar = Ph, Ar′ = 2-BrC_6H_4; **3c**, Ar = Ph, Ar′ = 2-$CF_3C_6H_4$) are obtained by the reaction of Ar′$CN_2(SiMe_3)_3$ with 3 molar equivs of ArSCl in CH_2Cl_2. X-ray structural determinations have shown that **1d** exists as a *Z,E,Z* isomer with a weak intramolecular S···N interaction [2.607(10) Å], whereas **3b** adopts an *E,E,E* configuration. Crystals of **1d** are monoclinic, space group $P2_1/n$, with a = 6.140(2) Å, b = 10.492(6) Å, c = 20.728(9) Å, β = 96.56(4)°, V = 1325(1) Å^3, Z = 2, R = 0.056, and R_w = 0.052. Crystals of **3b** are orthorhombic, space group *Ccca*, with a = 13.884(5) Å, b = 24.763(7) Å, c = 14.500(3) Å, V = 4985(2) Å^3, Z = 8, R = 0.043, and R_w = 0.044. Density functional theory calculations for the model diazenes HEN═C(H)N═NC(H)═NEH (E = S, Se, Te) show that (a) *Z,E,Z* isomers with an intramolecular E···N interaction are more stable than the *E,E,E* isomers, (b) the intramolecular interaction involves donation from the σ(N) lone pairs into both σ*(S−H) and σ*(S−N) and back-donation from a chalcogen π lone pair into the π*(N═N) orbital, and (c) the intense visible absorption bands (λ_{max} 500−550 nm, $\epsilon = 1 \times 10^4$ M^{-1} cm^{-1}) can be attributed to the π-HOMO ($3a_u$) → π*-LUMO ($3b_g$) transition. Variable-temperature ^{1}H NMR spectra of PhSN═C(H)N═NC(H)═NSPh in toluene-d_8 and in CD_2Cl_2 provide evidence for the co-existence and interconversion of several geometrical isomers.

Introduction

Intramolecular interactions are known to have an important influence on the structures, properties, and reactivity of certain chalcogen−nitrogen compounds.[1,2] For example, a sulfur(II) center involved in an interannular contact with nitrogen displays a remarkable inertness toward oxidation with *m*-chloroperbenzoic acid.[3] On the other hand, Se···N interactions are thought to play an important role in the reduction of peroxides by glutathione peroxidase, an essential selenium-containing antioxidant enzyme.[4]

Several years ago we described the formation of chalcogen-containing diazenes of the type **1**.[5,6] An X-ray structure of **1a**

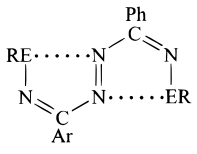

1a (E = Se, R = Me, Ar = Ph)
1b (E = Se, R = Ar = Ph)
1c (E = S, R = Ar = Ph)
1d (E = S, R = Ar = 4-$CH_3C_6H_4$)

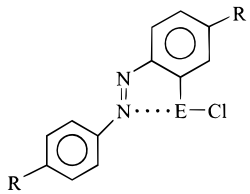

2a (E = Se, R = Me)
2b (E = Te, R = H)

revealed a planar *Z,E,Z* structure and a weak, intramolecular Se···N contact of 2.65 Å.[5] Very recently, a related, but much stronger, selenium−diazene interaction [d(Se···N) = 2.025 Å] has been reported for the selenenyl halide **2a**.[7] Intramolecular Te···N interactions are a common feature in organotellurium compounds, including ortho-tellurated azobenzenes.[2] Indeed such interactions stabilize tellurium(II) compounds of the type ArTeCl, e.g. **2b** [d(Te−N) = 2.19(2) and 2.23(2) Å].[8] Typical distances for S−N, Se−N, and Te−N single bonds are 1.73, 1.86, and 2.05 Å, respectively.[9] The sums of covalent radii for S and N, Se and N, and Te and N are 3.35, 3.50, and 3.75 Å, respectively.[9]

In contrast to the structure established for **1a**, the azo dialdehyde dioxime **3a** (an oxygen analogue of **1a**) has an *E,E,E*

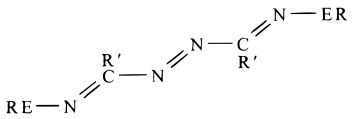

3a (E = O, R = R′ = H)
3b (E = S, R = Ph, R′ = 2-BrC_6H_4)
3c (E = S, R = Ph, R′ = 2-$CF_3C_6H_4$)

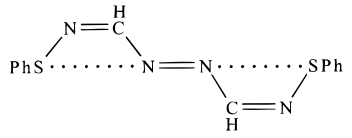

4

configuration that minimizes the repulsion between multiple lone pairs.[10] No other geometrical isomers of **3a** have been structur-

[⊗] Abstract published in *Advance ACS Abstracts,* September 1, 1996.

(1) (a) Kuszman, A.; Kapovits, L. In *Organic Sulfur Chemistry: Theoretical and Experimental Advances*; Csizmadia, I. G., Mangini, A., Eds.; Elsevier: Amsterdam, 1985; p 191. (b) Hargittai, I.; Rozsondai, R. In *The Chemistry of Organic Selenium and Tellurium Compounds*; Patai, S., Rappoport, Z., Eds.; Wiley: New York, 1986; Vol. 1, p 63.
(2) For examples of intramolecular Te···N coordination, see: (a) Sudha, N.; Singh, H. B. *Coord. Chem. Rev.* **1994**, *135/136*, 469. (b) Kaur, R.; Singh, H. B.; Butcher, R. J. *Organometallics* **1995**, *14*, 4755.
(3) Dunn, P. J.; Rees, C. W.; Slawin, A. M. Z.; Williams, D. J. *J. Chem. Soc., Chem. Commun.* **1989**, 1134.
(4) (a) Tomoda, S.; Iwaoka, M. In *Unusual Valency and Property of Organic Compounds of Main Group Elements*; Akiba, K., Ed.; Hiroshima University: Hiroshima, Japan, 1993; p 163. (b) Wilson, S. R.; Zucker, P. A.; Huang, R.-R. C.; Spector, A. *J. Am. Chem. Soc.* **1989**, *111*, 5936. (c) Engman, L.; Stern, D.; Cotgreave, I. A.; Andersson, C. M. *J. Am. Chem. Soc.* **1992**, *114*, 9737.
(5) Chandrasekhar, V.; Chivers, T.; Fait, J. F.; Kumaravel, S. S. *J. Am. Chem. Soc.* **1990**, *112*, 5373.

S0020-1669(96)00465-X CCC: $12.00

ally characterized. Since sulfur derivatives of the type **1** exhibit intense visible absorption bands similar to those of their Se analogues (λ_{max} 500−550 nm, $\epsilon \geq 1 \times 10^4$ L mol^{-1} cm^{-1}),[6,7] it has been assumed that they are also structurally related, but no X-ray structures have been reported. Very recently, however, we have isolated and determined the solid-state structure of an alternative *Z,E,Z* isomer, **4**.[11] The structure of **4** is related to that of **1c** by rotation about the C−N single bonds so that the intramolecular S···N interaction (2.83 Å)[11] gives rise to a four-membered ring rather than a five-membered ring. The structure determinations for the chalcogen-substituted diazenes **1a** and **4**[11] indicate essentially localized bonding, i.e. two C═N double bonds and one N═N double bond. Thus it is evident that a variety of geometrical isomers is possible for this class of compounds.

These considerations raise a number of important questions about the structures and properties of this interesting class of diazenes: (a) What are the relative stabilities of the various possible geometrical and conformational isomers? (b) Is it possible to isolate and structurally characterize other geometrical isomers? (c) Can these isomers undergo interconversion? (d) What is the nature of the intramolecular E···N interaction, and why is it so much stronger in the halogeno derivative **2a** compared to **1a**? Approximate density functional theory (DFT) has proven to be an efficient method for modeling the structures and properties of chalcogen−nitrogen compounds.[11−13] In this paper we report the X-ray structures of the *Z,E,Z* isomer **1d** and the *E,E,E* isomer **3b** and we address questions (a) and (c) by means of DFT theory.

Experimental Section

Reagents and General Procedures. All reactions and the manipulation of moisture-sensitive compounds were carried out under an atmosphere of dry N_2 by using Schlenk techniques. The following compounds were prepared by literature procedures: PhSN═C(H)-N═NC(H)═NSPh,[11] 2-$XC_6H_4CN_2(SiMe_3)_3$ (X = CF_3, Br).[14] The reagents ArSCl (Ar = Ph, 4-$CH_3C_6H_4$) were obtained by the treatment of Ar_2S_2 (Aldrich) with SO_2Cl_2 in CCl_4. All solvents were dried with the appropriate reagents and distilled before use.

Instrumentation. UV−visible spectra were obtained by using a Cary 5E spectrophotometer. ^{1}H NMR spectra were recorded on Bruker ACE 200 and AMX 400 spectrometers; chemical shifts are reported relative to Me_4Si. Elemental analyses were obtained by the Analytical Services division of the Department of Chemistry, The University of Calgary.

Preparation of ArSN═C(Ar)N═NC(Ar)═NSAr, 1d (Ar = 4-$CH_3C_6H_4$). A solution of 4-$CH_3C_6H_4CN_2(SiMe_3)_3$ (0.550 g, 1.57 mmol) in CH_2Cl_2 (25 mL) was added to a solution of *p*-toluenesulfenyl chloride (0.746 g, 4.70 mmol) in CH_2Cl_2 (25 mL) at −78 °C. The purple solution was stirred at 23 °C for 1 h. Removal of solvent and volatile products under vacuum yielded a purple solid residue which was extracted with pentane (2 × 30 mL) to give di-*p*-tolyl disulfide (0.30 g, 1.22 mmol, 75%). The purple product was recrystallized from diethyl ether and identified as 4-$CH_3C_6H_4SN$(4-$CH_3C_6H_4$)CN═$NC(C_6H_4$-CH_3-4)$NSC_6H_4CH_3$-4 (0.28 g, 0.55 mmol, 72%), mp 112−114 °C. Anal. Calcd for $C_{30}H_{28}N_4S_2$: C, 70.83; H, 5.55; N, 11.01. Found: C, 70.07; H, 5.59; N, 10.85. ^{1}H NMR ($CDCl_3$): δ 7.3−8.3 (two AB quartets, C_6H_4, 8), 2.47 (s, $C_6H_4CH_3$, 3), 2.41 (s, $C_6H_4CH_3$, 3). ^{13}C NMR ($CDCl_3$): 198.5 (*C*N═N*C*), 138.6, 131.6, 129.8, 129.5, 129.1, 127.8, 127.4, 125.3 ($CH_3C_6H_4$), 21.50 ($CH_3C_6H_4S$), 21.22 ($CH_3C_6H_4C$). UV−vis (CH_2Cl_2): λ_{max} 550 nm, $\epsilon = 1.79 \times 10^4$ M^{-1} cm^{-1}.

Preparation of PhSN═C(2-BrC_6H_4)N═NC(2-BrC_6H_4)═NSPh, 3b. A solution of PhSCl (1.89 g, 13.3 mmol) in CH_2Cl_2 (70 mL) was added dropwise (45 min) to a solution of 2-$BrC_6H_4CN_2(SiMe_3)_3$ (1.85 g, 4.46 mmol) in CH_2Cl_2 (90 mL) at −100 °C. The reaction mixture was kept at −78 °C for 16 h, and then solvent and Me_3SiCl were removed under vacuum. The solid residue was extracted with pentane (5 × 20 mL), and the pentane-soluble products were separated on a silica column (130−270 mesh, column size 2.5 × 40 cm) by elution with hexane to give Ph_2S_2 (0.72 g, 3.30 mmol, 74%) and red prisms of PhSN═C(2-BrC_6H_4)N═NC(2-BrC_6H_4)═NSPh (0.68 g, 50%), mp 178−9 °C, after recrystallization from CH_2Cl_2 at −20 °C. Anal. Calcd for $C_{26}H_{18}Br_2N_4S_2$: C, 51.16; H, 2.97; N, 9.18. Found: C, 50.88; H, 2.96; N, 9.03. ^{1}H NMR ($CDCl_3$): δ 7.2−7.8 (m, C_6H_5 and C_6H_4) and 7.9 (d, C_6H_4). UV−vis (CH_2Cl_2): λ_{max} 469 nm, $\epsilon = 1.75 \times 10^4$ M^{-1} cm^{-1}.

Preparation of PhSN═C(2-$CF_3C_6H_4$)N═NC(2-$CF_3C_6H_4$)═NSPh, 3c. Compound **3c** was obtained as red crystals in 25% yield after recrystallization (CH_2Cl_2−diethyl ether) from the reaction of 2-$CF_3C_6H_4$-$CN_2(SiMe_3)_3$ with PhSCl (1:3 molar ratio) by using the procedure outlined for **3b**. Anal. Calcd for $C_{28}H_{18}F_6N_4S_2$: C, 57.14; H, 3.08; N, 9.52. Found: C, 56.75; H, 2.87; N, 9.11. ^{1}H NMR ($CDCl_3$): δ 7.26−7.88 (m, C_6H_5 and C_6H_4). UV−vis (CH_2Cl_2): λ_{max} 469 nm, $\epsilon = 1.57 \times 10^4$ M^{-1} cm^{-1}.

X-ray Analyses. All measurements were made on a Rigaku AFC6S diffractometer with graphite monochromated Mo Kα radiation (λ = 0.710 69 Å). The crystal data for **1d** and **3b** are given in Table 1, and atomic coordinates for **1d** and **3b** can be found in Tables 2 and 3, respectively.

1d. A purple plate (0.08 × 0.20 × 0.42 mm) was obtained by recrystallization from diethyl ether at −20 °C and mounted on a glass fiber. Accurate cell dimensions and a crystal orientation matrix were obtained by a least-squares fit of the setting angles of 25 reflections. The data were corrected for Lorentz, polarization, and empirical absorption effects.[15] The structure was solved by direct methods using SAPI91.[16] Refinement of the structure was by full-matrix least-squares calculations, initially with isotropic and finally with anisotropic temperature factors for the non-H atoms; phenyl rings were allowed to refine as regular hexagons. At an intermediate stage in the refinement,

Table 1. Crystallographic Data for **1d** and **3b**

	1d	**3b**
formula	$C_{30}H_{28}N_4S_2$	$C_{26}H_{18}N_4S_2Br_2$
fw	508.70	610.38
cryst system	monoclinic	orthorhombic
space group	$P2_1/n$ (No. 14)	*Ccca* (No. 68)
a, Å	6.140(2)	13.884(5)
b, Å	10.492(6)	24.763(7)
c, Å	20.728(9)	14.500(3)
β, deg	96.56(4)	
Z	2	8
V, Å^3	1325(1)	4985(2)
ρ_{calcd}, g cm^{-3}	1.275	1.626
F(000)	536	2432
μ, cm^{-1}	2.27	34.52
no. unique reflcns	2495	2462
no. reflcns ($I > 3.00\sigma$(I))	638	736
T, °C	−53.0	−123.0
R^a	0.056	0.043
$R_w{}^b$	0.052	0.044

^{a} $R = \sum||F_o| - |F_c||/\sum|F_o|$. ^{b} $R_w = [\sum w\Delta^2/\sum wF_o{}^2]^{1/2}$.

(6) Chandrasekhar, V.; Chivers, T.; Kumaravel, S. S.; Parvez, M.; Rao, M. N. S. *Inorg. Chem.* **1991**, *30*, 4125.
(7) Jones, P. G.; Ramirez de Arellano, M. C. *Chem. Ber.* **1995**, *128*, 741.
(8) Cobbledick, R. E.; Einstein, F. W. B.; McWhinnie, W. R.; Musa, F. H. *J. Chem. Res. (S)* **1979**, 145; *J. Chem. Res.* (*M*) **1979**, 1901.
(9) (a) Pauling, L. *The Nature of the Chemical Bond*, 3rd ed.; Cornell University Press, Ithaca, NY, 1960. (b) Björgvinsson, M.; Roesky, H. W. *Polyhedron* **1991**, *10*, 2353.
(10) Bois, C.; Armand, J.; Bassinet, P. *Acta Crystallogr.* **1980**, *B36*, 1731.
(11) Chivers, T.; McGarvey, B.; Parvez, M.; Vargas-Baca, I.; Ziegler, T. *Inorg. Chem.* **1996**, *35*, 3839.
(12) Chivers, T.; McGregor, K.; Parvez, M.; Vargas-Baca, I.; Ziegler, T. *Can. J. Chem.* **1995**, *73*, 1380.
(13) Chivers, T.; Jacobsen, H.; Vollmerhaus, R.; Ziegler, T. *Can. J. Chem.* **1994**, *72*, 1582.
(14) Boeré, R. T.; Oakley, R. T.; Reed, R. W. *J. Organomet. Chem.* **1987**, *331*, 161.
(15) North, A. C. T.; Phillips, D. C.; Mathews, F. S. *Acta Crystallogr.* **1968**, *A24*, 351.
(16) Fan, H.-F. SAPI91: Structure Analysis Programs with Intelligent Controls, Rigaku Corp., Tokyo, Japan, 1991.

Table 2. Atomic Coordinates and B_{eq} (Å^2) Values for **1d**

atom	*x*	*y*	*z*	B_{eq}[a]
S(1)	0.3769(5)	0.0777(3)	0.6192(1)	3.2(2)
N(1)	0.2365(13)	−0.0380(8)	0.5809(4)	2.6(4)
N(2)	0.4311(13)	−0.0397(8)	0.4850(4)	2.6(4)
C(1)	0.2075(9)	0.1114(7)	0.6812(4)	2.5(5)
C(2)	0.2837(9)	0.2090(7)	0.7236(4)	3.3(6)
C(3)	0.1622(9)	0.2458(7)	0.7734(4)	4.2(6)
C(4)	−0.0354(9)	0.1849(7)	0.7808(4)	3.3(6)
C(5)	−0.1116(9)	0.0873(7)	0.7384(4)	3.3(6)
C(6)	0.0099(9)	0.0505(7)	0.6886(4)	3.2(5)
C(7)	−0.1668(16)	0.2255(11)	0.8352(5)	4.5(7)
C(8)	0.2716(15)	−0.0824(12)	0.5242(5)	2.9(5)
C(9)	0.1340(9)	−0.1903(7)	0.4958(3)	1.9(4)
C(10)	0.1906(9)	−0.2563(7)	0.4417(3)	3.2(5)
C(11)	0.0574(9)	−0.3551(7)	0.4150(3)	3.6(6)
C(12)	−0.1323(9)	−0.3878(7)	0.4423(3)	3.2(6)
C(13)	−0.1889(9)	−0.3217(7)	0.4963(3)	4.1(7)
C(14)	−0.0557(9)	−0.2230(7)	0.5231(3)	3.8(6)
C(15)	−0.2850(18)	−0.4922(11)	0.4119(5)	5.4(7)

[a] $B_{eq} = {}^8/_3\pi^2(U_{11}(aa^*)^2 + U_{22}(bb^*)^2 + U_{33}(cc^*)^2 + 2U_{12}aa^*bb^* \cos\gamma + 2U_{13}aa^*cc^* \cos\beta + 2U_{23}bb^*cc^* \cos\alpha)$.

Table 3. Atomic Coordinates and B_{eq} Values (Å^2) for **3b**

atom	*x*	*y*	*z*	B_{eq}[a]
Br(1)	0.85117(9)	0.33354(6)	0.16165(9)	4.46(3)
S(1)	0.6322(2)	0.4214(1)	0.2179(2)	2.66(7)
N(1)	0.6339(5)	0.2710(3)	0.2743(5)	1.7(2)
N(2)	0.6280(6)	0.3637(3)	0.2713(5)	2.3(2)
C(1)	0.6373(7)	0.3191(4)	0.2224(6)	1.8(3)
C(2)	0.6530(9)	0.3172(4)	0.1194(6)	1.8(2)
C(3)	0.7441(9)	0.3223(4)	0.0840(7)	2.0(2)
C(4)	0.7602(8)	0.3186(4)	−0.0097(8)	2.7(3)
C(5)	0.6826(9)	0.3106(5)	−0.0659(7)	2.9(3)
C(6)	0.5901(9)	0.3054(5)	−0.0320(7)	3.1(3)
C(7)	0.5728(8)	0.3093(4)	0.0611(7)	1.9(3)
C(8)	0.6217(8)	0.4659(4)	0.3098(7)	2.1(3)
C(9)	0.6231(10)	0.4508(5)	0.4007(8)	4.2(4)
C(10)	0.6191(10)	0.4902(5)	0.4670(7)	5.0(4)
C(11)	0.6113(11)	0.5429(5)	0.4455(8)	4.7(4)
C(12)	0.6099(9)	0.5580(4)	0.3538(8)	4.2(4)
C(13)	0.6172(8)	0.5182(5)	0.2863(7)	3.6(3)

[a] $B_{eq} = {}^8/_3\pi^2(U_{11}(aa^*)^2 + U_{22}(bb^*)^2 + U_{33}(cc^*)^2 + 2U_{12}aa^*bb^* \cos\gamma + 2U_{13}aa^*cc^* \cos\beta + 2U_{23}bb^*cc^* \cos\alpha)$.

a difference map revealed maxima consistent with the positions of H atoms which were included in the subsequent cycles of refinement at geometrically idealized positions (C−H 0.95 Å) with an overall isotropic temperature which was allowed to refine. In the refinement cycles, weights were derived from the counting statistics. Scattering factors were taken from refs 17 and 18, and allowance was made for anomalous dispersion.[19] Refinements were carried out using SHELX 76,[20] and the computer programs used for data reduction and structure solution were part of the teXsan package.[21]

3b. A dark orange prismatic crystal of **3b** (0.55 × 0.45 × 0.40 mm) obtained by recrystallization from dichloromethane was mounted on a glass fiber. Cell constants and an orientation matrix for data collection were obtained from a least-squares refinement using the setting angles of 25 carefully centered reflections in the range $15.00 < 2\theta < 30.00°$. A linear correction factor was applied to the data to account for a 0.8% decrease in the standards over the course of the data collection. An empirical absorption correction was applied, and the data were corrected for Lorentz and polarization effects. The structure was solved by direct methods[22] and expanded using Fourier techniques.[23] The non-H atoms were refined anisotropically. Hydrogen atoms were included but not refined. Scattering factors were taken from ref 24, and allowance was made for anomalous dispersion.[25]

Computational Details

All calculations were based on approximate density functional theory (DFT) within the local density approximation,[26] using the ADF program system developed by Baerends et al.,[27,28] and vectorized by Raveneck.[29] The numerical integration was based on a scheme developed by Becke.[30] All molecular dimensions were fully optimized, by a procedure based on the method developed by Versluis and Ziegler.[31] All atomization energies [total atomization energy = E(molecule) − ΣE(free atoms)] were evaluated by the generalized transition state method due to Ziegler and Rauk.[32] This treatment also allowed for a detailed energy decomposition of the total bonding energy into steric (electrostatic, $\delta_{\text{exchange-correlation}}$, electron-exchange repulsion) and single orbital contributions.[33] A double-ζ STO basis[34] was employed for the *n*s and *n*p shells of the main group elements. This basis was augmented by a 3d STO function for sulfur, 4d STO for selenium, and 5d STO for tellurium, and for hydrogen a 2p STO was used as polarization. Electrons in lower shells were treated by the frozen core approximation.[27] A set of auxiliary[35] s, p, d, f, and g STO functions, centered on the different nuclei, was used in order to fit the molecular density and present Coulomb and exchange potentials accurately in each SCF cycle. Energy differences were calculated by augmenting the local density approximation (LDA) energy expression by Vosko et al.[36] with Becke's[37] exchange corrections and Perdew's nonlocal correlation correction.[38]

Results and Discussion

Preparation and X-ray Structures of 1d and 3b. The diazenes **1d**, **3b**, and **3c** were obtained in 72%, 50%, and 25% yields, respectively, from the reaction of the appropriate trisilylated benzamidine with 3 molar equivs of ArSCl in CH_2Cl_2 at low temperatures (eq 1). The diazene **1d** is a dark purple

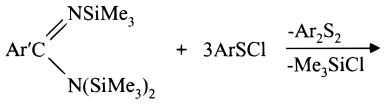

$$\tfrac{1}{2}\text{ArSN=C(Ar')N=NC(Ar')=NSAr} \quad (1)$$

(**1d**, Ar = Ar′ = 4-$CH_3C_6H_4$)

(**3b**, Ar′ = 2-BrC_6H_4, Ar = Ph)

(**3c**, Ar′ = 2-$CF_3C_6H_4$, Ar = Ph)

solid with a characteristic visible absorption band at 550 nm,[6] whereas **3b**,**c** form dark red crystals, λ_{max} *ca*. 470 nm. Significantly, a dark (burgundy) red product, in addition to the

(17) Cromer, D. T.; Mann, J. B. *Acta Crystallogr.* **1968**, *A24*, 321.
(18) Stewart, R. F.; Davidson, E. R.; Simpson, W. T. *J. Chem. Phys.* **1965**, *42*, 3175.
(19) Cromer, D. T.; Libermann, D. *J. Chem. Phys.* **1970**, *53*, 1891.
(20) Sheldrick, G. M. SHELX76. Program for Crystal Structure Determination. University of Cambridge, England, 1976.
(21) teXsan Single Crystal Structure Analysis Software, Molecular Structure Corp., The Woodlands, TX 77381, 1993.
(22) SIR92: Altomare, A.; Burla, M. C.; Camalli, M.; Cascarano, M.; Giacovazzo, C.; Guagliardi, A.; Polidori, G. *J. Appl. Crystallogr.*, manuscript in preparation.
(23) DIRDIF94: Beurskens, P. T.; Admiraal, G.; Beurskens, G.; Bosman, W. P.; de Gelder, R.; Israel, R.; Smits, J. M. M. (1994). The DIRDIF-94 program system, Technical Report of the Crystallography Laboratory, University of Nijmegen, The Netherlands, 1994.
(24) Cromer, D. T.; Waber J. T. *International Tables for X-ray Crystallography*; Vol. IV, The Kynoch Press: Birmingham, England, 1994; Vol. IV, Table 2.2 A.
(25) Ibers, J. A.; Hamilton, W. C. *Acta Crystallogr.* **1964**, *17*, 781.
(26) (a) Gunnarsson, O.; Lundquist, I. *Phys. Rev.* **1974**, *B10*, 1319. (b) Gunnarsson, O.; Lundquist, I. *Phys. Rev.* **1976**, *B13*, 4274. (c) Gunnarsson, O.; Johnson, M.; Lundquist, I. *Phys. Rev.* **1979**, *B20*, 3136.
(27) Baerends, E. J.; Ellis, D. E.; Ros, P. *Chem. Phys.* **1973**, *2*, 41.
(28) Baerends, E. J. Ph.D. Thesis, Frije Universiteit, Amsterdam, 1975.
(29) Ravenek, W. In *Algorithms and Applications on Vector and Parallel Computers*; Riele, H. J. J., Dekker, Th. J., van de Horst, H. A., Eds.; Elsevier: Amsterdam, 1987.
(30) Becke, A. D. *J. Chem. Phys.* **1988**, *88*, 2547.
(31) Versluis, L.; Ziegler, T. *J. Chem. Phys.* **1988**, *88*, 322.
(32) Ziegler, T.; Rauk, A. *Theor. Chim. Acta* **1977**, *46*, 1.

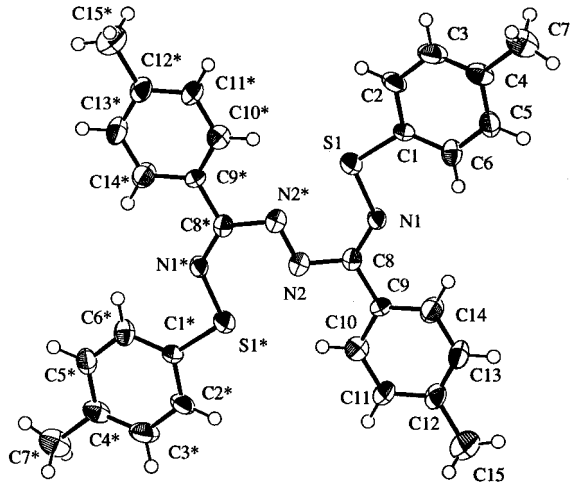

Figure 1. ORTEP drawing of ArSN═CArN═NCAr═NSAr, **1d** (Ar = 4-$CH_3C_6H_4$).

purple diazene, has been observed in the separation of the products from eq 1 (Ar′ = 4-BrC_6H_4, Ar = Ph) by TLC, but it quickly transforms into the purple diazene and cannot be isolated.[39]

In order to establish whether the distinctly different colors of the sulfur(II)-containing diazenes **1d** and **3b**/**3c** are indicative of a specific geometrical isomer, the X-ray structures of two derivatives were determined. ORTEP drawings of **1d** and **3b** with the appropriate numbering scheme are displayed in Figures 1 and 2, respectively. The diazene **1d** adopts the planar *Z*,*E*,*Z* structure previously established for the selenium analogue **1a**.[5] By contrast, **3b** exists as the *E*,*E*,*E* isomer. The bond lengths and bond angles for the essentially planar SNCNNCNS chains in the three sulfur-substituted diazenes **1d**, **3b**, and **4** are compared in Table 4. The bond lengths for all three derivatives indicate essentially localized bonding with C−N single bonds in the range 1.39−1.41 Å, C═N double bonds in the range 1.30−1.32 Å, and an N═N double bond with a value 1.25−1.29 Å (cf. 1.25 Å for azobenzenes).[40] The 2-BrC_6H_4 groups in **3b** lie in a plane perpendicular to the SNCNNCNS chain. It is possible that the steric effect of the *ortho* substituent impedes the conversion to the thermodynamically more stable *Z*,*E*,*Z* isomer in the case of **3b** (*vide infra*). Significantly, the longest −N═N− bond [1.294(14) Å] is observed for **1d** in which the intramolecular S···N interaction [2.607(10) Å] is significantly stronger than the value of 2.83(1) Å observed for **4**.[11]

Geometrical Isomers of HSN═C(H)N═NC(H)═NSH: Relative Stabilities. In order to gain some insight into the relative stabilities of the geometrical isomers of the model diazene HSN═C(H)N═NC(H)═NSH DFT calculations were carried out for the five structures shown in Figure 3: **I** and **II** are *Z*,*E*,*Z* isomers, while **III**−**V** are *E*,*E*,*E*. The pair of *Z*,*E*,*Z* isomers **I** and **II** and the pair of *E*,*E*,*E* isomers **III** and **IV** are rotamers related to each other by rotation about the C−N single bonds. In view of the preference of diazenes for a *trans*(*E*) geometry,[41] isomers with a *cis*(*Z*) orientation at the −N═N− bond were not considered. All structures were fully optimized by assuming C_{2h} symmetry. A total bonding energy analysis showed that isomer **I** (cf. **1d**) is the most stable. However, isomer **II** (cf. **4**) is only 17.4 kJ mol^{-1} higher in energy than I for the model system and isomer **III** (cf. **3b**) is 27.2 kJ mol^{-1} above **I**. Thus, examples of the three most stable geometrical isomers of these sulfur-containing diazenes have now been isolated and structurally characterized. The electronic structures of the model diazene confirm the previously proposed assignment of the intense color of these compounds to the first symmetry-allowed electronic transition π-HOMO ($3a_u$) → π^*-LUMO ($3b_g$).[6]

The calculated molecular dimensions of the isomers **I**−**V** are compared with experimental data for **1a**, **3b**, and **4** in Table 4.

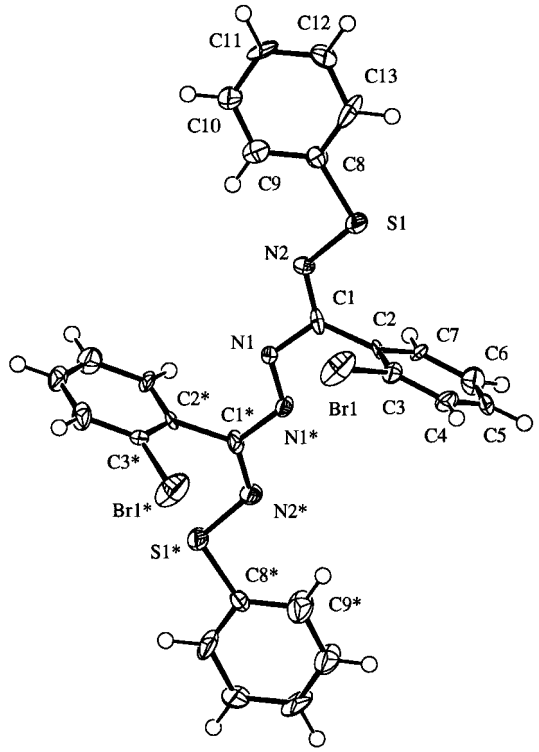

Figure 2. ORTEP drawing of PhSN═C(2-BrC_6H_4)N═NC(2-BrC_6H_4)═NSPh, **3b**.

Table 4. Comparison of Selected Bond Lengths (Å) and Bond Angles (deg) for **1d**, **3b**, and **4** and the Models **I**−**V**

	1d	I	4[a]	II	3b	III	IV	V
Bond Lenghts								
N═N	1.294(14)	1.277	1.254(8)	1.292	1.26(1)	1.285	1.277	1.272
N−C	1.415(11)	1.367	1.392(7)	1.377	1.41(1)	1.381	1.363	1.393
C═N	1.303(11)	1.290	1.296(7)	1.296	1.32(1)	1.293	1.286	1.274
N−S	1.641(8)	1.680	1.658(5)	1.706	1.627(8)	1.696	1.646	1.672
S−C	1.779(7)		1.780(5)		1.74(1)			
N···S	2.607(10)	2.448	2.83(1)	2.946				
Bond Angles								
NSC	100.3(4)		100.2(3)		100.9(5)			
SNC	124.7(7)	121.1	118.0(2)	120.0	118.5(6)	118.2	122.8	117.0
NCN	126.9(10)	126.9	122.4(5)	124.5	114.7(8)	115.0	118.4	124.9
CNN	112.2(7)	112.6	112.4(6)	112.2	113.5(9)	111.7	112.5	115.0

[a] Data taken from ref 11.

(33) Ziegler, T. In *Metal-Ligand Interactions: from Atoms, to Clusters, to Surfaces*; Salahub, D. R., Russo, N., Eds.; Kluwer Academic Publishers: Amsterdam, 1992.
(34) (a) Snijders, J. G.; Baerends, E. J.; Vernoijs, P. *At. Nucl. Data Tables* **1982**, *26*, 483. (b) Vernoijs, P.; Snijders, J. G.; Baerends, E. J. *Slater Type Basis Functions for the Whole Periodic System, Internal Report*; Frije Universiteit: Amsterdam, 1981.
(35) Krijn, J.; Baerends, E. J. *Fitfunctions in the HFS Method, Internal Report*; Frije Universiteit: Amsterdam, 1984.
(36) Vosko, S. H.; Wilk, L.; Nusair, M. *Can. J. Phys.* **1990**, *58*, 1200.
(37) Becke, A. D. *J. Phys. Rev. A* **1988**, *38*, 2938.
(38) (a) Perdew, J. P. *Phys. Rev.* **1986**, *B33*, 8822. (b) Perdew, J. P. *Phys. Rev.* **1986**, *B34*, 7406.
(39) Chivers, T.; Zoricak, P. Unpublished results.
(40) Hope, H.; Victor, D. *Acta Crystallogr.* **1969**, *B25*, 1849.
(41) Allman, R. In *The Chemistry of the Hydrazo, Azo and Azoxy Groups*, Patai, S., Ed.; John Wiley and Sons: New York, 1975; Chapter 2.

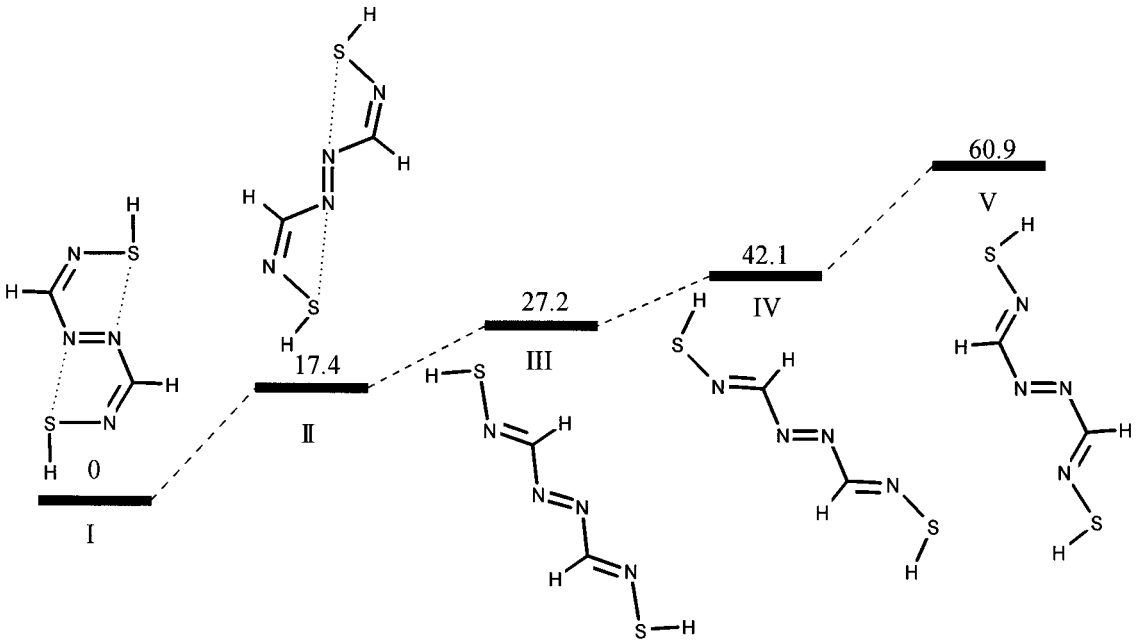

Figure 3. Relative energies (kJ mol^{-1}) of geometrical isomers of HSN═C(H)N═NC(H)═NSH.

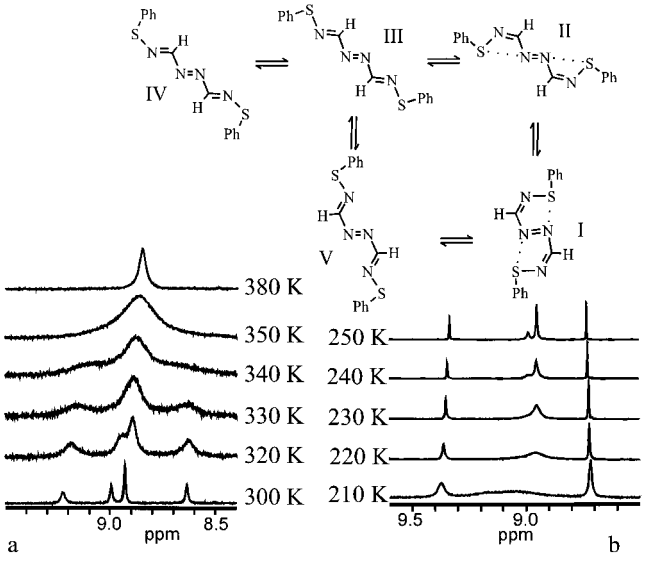

Figure 4. Variable-temperature ^{1}H NMR spectra of PhSN═C(H)N═NC(H)═NSPh in (a) toluene-d_8 and (b) dichloromethane-d_2.

Although there is reasonably good agreement between the calculated and experimental data, this comparison is of limited value in view of the inability of the model system to mimic the steric and/or electronic effects of the substituents on C and S in **1a**, **3b**, and **4**.

Variable-Temperature ^{1}H NMR Spectra of PhSN═C(H)N═NC(H)═NSPh (4). Evidence for the co-existence and interconversion of several geometrical isomers of PhSN═C(H)N═NC(H)═NSPh (**4**) in solution has been obtained from VT ^{1}H NMR studies in toluene-d_8 and CD_2Cl_2. As indicated in Figure 4a, the ^{1}H NMR spectrum of **4** in toluene-d_8 at 300 K displays four singlets in the region δ 8.5−9.5. This spectrum is reproducibly obtained for different samples of **4**. The relative intensities of these four resonances are independent suggesting that each one corresponds to the formamidinic proton of a symmetrical, geometrical isomer of **4**. Upon heating of the solution the middle two signals broaden and coalesce at 330 K, while the outer two signals also broaden. At higher temperatures all four resonances collapse to give a singlet. It is proposed that these observations may be attributed to exchange between the *E*,*E*,*E* rotamers **III** and **V** (via C−N bond rotation) and, subsequently, an exchange with the *Z*,*E*,*Z* isomers **I** and **II**. The higher energy of this second exchange process is ascribed to the intramolecular S···N interactions in **I** and **II**. The reverse of these changes is observed upon cooling the solution to 300 K.

^{1}H NMR spectra of **4** below room temperature revealed a second exchange process. As indicated in Figure 4b these spectra were recorded in CD_2Cl_2 owing to the limited solubility of **4** in toluene-d_8. Small changes in chemical shifts are observed on changing the solvent, but the overall appearance of the NMR spectrum is unaltered. On cooling of the solution, the outer two resonances do not change consistent with the assignment of these signals to the thermodynamically most stable isomers **I** and **II** (*vide supra*). However, the middle two resonances broaden to give a new set of poorly resolved signals at 210 K indicating that a very low energy exchange process is occurring even at this temperature. It is tentatively suggested that this process involves rotation about the S−N single bonds in the way that the rotamers **III** and **IV** are related. The reverse of these changes is observed on warming the solution to room temperature.

Intramolecular Chalcogen−Nitrogen Interactions in *Z*,*E*,*Z*-HSN═C(H)N═NC(H)═NSH. It is apparent from the DFT calculations that the intramolecular S···N interactions observed for the *Z*,*E*,*Z* isomers **1d** and **4** have a stabilizing influence. Frequently this kind of "intramolecular coordination" is explained, on the basis of qualitative arguments, as donation of the nitrogen lone pair (σ(N)lp) into the σ*(S-X) orbitals (**5a**).[7]

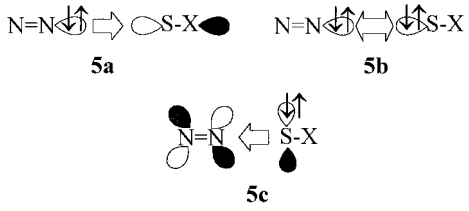

5a **5b**

5c

However, this simplistic picture neglects a lone pair of the chalcogen (σ(S)lp) which also has an orientation suitable to

Table 5. Calculated Contributions to the Total Atomization Energy (kJ mol^{-1}) of the Exchange Repulsions and Orbital Interactions for the Model Diazenes HEN═C(H)N═N(H)C═NEH (Corrections Not Included)

	E = S			E = Se			E = Te		
	geometry			geometry			geometry		
	I	V	Δ	I	V	Δ	I	V	Δ
				Exchange Repulsion (ER)					
A_g	17217.5	16849.7		16612.5	16325.1		16473.8	15987.1	
B_g	240.5	264.8		222.3	238.4		216.4	234.2	
A_u	852.3	806.2		824.9	787.6		814.8	764.9	
B_u	14746.8	14666.9		14160.2	14112.0		13967.8	13818.9	
				Orbital Interaction (OI)					
A_g	−11917.0	−11740.6		−11416.8	−11249.3		−11242.3	−10933.3	
B_g	−1406.8	−1409.8		−1346.4	−1346.3		−1319.8	−1309.5	
A_u	−2635.4	−2535.0		−2585.0	−2479.1		−2518.0	−2378.5	
B_u	−12272.5	−12275.1		−11744.3	−11811.4		−11517.2	−11543.5	
				ER + OI					
A_g	5300.5	5109.1	191.5	5195.7	5075.8	119.9	5231.5	5053.8	177.7
B_g	−1166.4	−1145.1	−21.3	−1124.1	−1107.8	−16.2	−1103.4	−1075.3	−28.1
A_u	−1783.1	−1728.9	−54.2	−1760.2	−1691.5	−68.7	−1703.1	−1613.6	−89.6
B_g	2474.3	2391.8	82.5	2416.0	2300.6	115.4	2450.6	2275.4	175.1
tot. at en	−6581.2	−6520.2	−61.0	−6369.0	−6294.6	−74.4	−6238.0	−6123.6	−114.4

Table 6. Population of Selected Fragment Orbitals in the Model Diazenes HEN═C(H)N═N(H)C═NEH

	E = S			E = Se			E = Te		
	geometry			geometry			geometry		
orbital	V	I	Δ	V	I	Δ	V	I	Δ
σ^*(H−E)A_u	0.01	0.06	0.05	0.04	0.09	0.05	0.05	0.07	0.02
σ^*(H−E)B_u	0.02	0.01	−0.01	0.07	0.01	−0.06	0.07	0.01	−0.06
σ^*(N−E)A_g	0.01	0.19	0.18	0.05	0.17	0.12	0.07	0.26	0.19
σ^*(N−E)B_u	0.01	0.08	0.07	0.04	0.09	0.05	0.08	0.30	0.22
π^*(N═N)B_g	0.29	0.47	0.18	0.31	0.49	0.18	0.31	0.58	0.27

interact repulsively with σ(N)lp (**5b**) and is even closer in energy to σ(N)lp than the σ^*(S−X) orbitals. Another neglected interaction is a π-"back-donation" of a chalcogen lone pair (π-(S)lp) into a suitable orbital, such as π^*(N═N) (**5c**).

This balance of forces was studied by comparing the contributions to the total atomization energy in models **I** and **V**. The exchange-repulsion and orbital-interaction contributions to the total energy are quoted in Table 5. Comparative analysis shows that while the σ interactions (a_g and b_u) are destabilizing the π(b_g and a_u) interactions stabilize **I** with respect to **V**. The same analysis was repeated for the model diazenes HEN═C(H)-N═NC(H)═NEH (E = Se, Te). The calculations showed that **I** is more stable than **V** by 74.4 and 114.4 kJ mol^{-1} for E = Se and Te, respectively. The model diazenes were split into the fragments $^{\bullet}$N═N$^{\bullet}$ and (HE-N═C(H)$^{\bullet}$)$_2$ to evaluate the extent of donation into the empty orbitals of each fragment (Table 6). Electron donation to both σ^*(E−H)(a_g and b_u) orbitals is negligible in all cases. Donation into π^*(N═N)(b_g) is considerable and increases for E = Te since the energy of π(Te)lp is closer to that of the acceptor orbital. Donation to σ^*(E−N)-(a_g) is also significant. Donation into σ^*(E−N)(b_u) becomes important only for E = Te. On the basis of this analysis, the chalcogen−diazene close contact is better described as a weak bonding interaction involving donation from a chalcogen lone pair π(E)lp to the π^*(N═N) orbital. The acceptor ability of the σ^*(S−X) orbitals of the SX_2 ligand in transition metal complexes is well established.[42] In the present case, however, the nitrogen lone pair is well below the energy of the metal valence electrons; consequently, the interaction with the σ^* levels is less effective and only alleviates the repulsive forces (Figure 5). Additional stabilization by the π(a_u) orbitals can be interpreted as the result of delocalization of electron density on two incipient five-membered rings.

It follows from the bonding description that intramolecular interactions of the type considered in this study would be enhanced by increasing the degree of donation into the π^*-(N═N) and/or σ^*(E−X) orbitals. Both of these effects are most pronounced for tellurium. Consequently, organotellurium compounds exhibit the strongest tendency toward intramolecular coordination.[3] On the other hand, the acceptor ability of the σ^*(E−X) is enhanced by increasing the electronegativity of X as evidenced by the examples **2a**[7] and **2b**.[8] Similar O···Se close contacts have been observed in the quinone derivatives **6a**, **6b** in which the O···Se distance is reduced from 2.575(3) to 2.079(3) Å by replacing the phenyl group with a chlorine atom.[43]

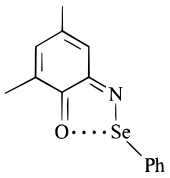

6a

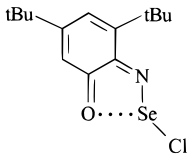

6b

The calculations indicate that intramolecular coordination should be even stronger for Te diazenes of the type **1** than that observed for the Se diazene **1a**.[6] However, an attempt to prepare a tellurium-containing diazene by the reaction of 4-$CH_3C_6H_4$-$CN_2(SiMe_3)_3$ with mesityltellurium bromide in CH_2Cl_2 resulted in recovery of the starting materials.[44]

Conclusions. A new structural isomer of the sulfur(II)-containing diazenes PhSN═C(Ar)N═NC(Ar)═NSPh (Ar = 2-BrC_6H_4) with an *E*,*E*,*E* geometry has been prepared and structurally characterized. The *E*,*E*,*E* isomers are dark red (λ_{max} 470 nm) whereas the *Z*,*E*,*Z* isomers exhibit deep purple colors (λ_{max} *ca.* 550 nm) and characteristic weak, intramolecular S···N contacts. DFT calculations indicate that the *Z*,*E*,*Z* isomers of the model chalcogen(II)-containing diazenes HEN═C(H)N═NC-(H)═NEH (E = S, Se, Te) are stabilized relative to the *E*,*E*,*E*

(42) Jacobsen, H.; Kraatz, H. B.; Ziegler, T.; Boorman, P. M. *J. Am. Chem. Soc.* **1992**, *114*, 7851.

(43) Roesky, H. W.; Weber, K.-L.; Seseke, U.; Pinkert, W.; Noltemeyer, M.; Clegg, W.; Sheldrick, G. M. *J. Chem. Soc., Dalton Trans.* **1985**, 565.

(44) Chivers, T.; Vargas-Baca, I. Unpublished results.

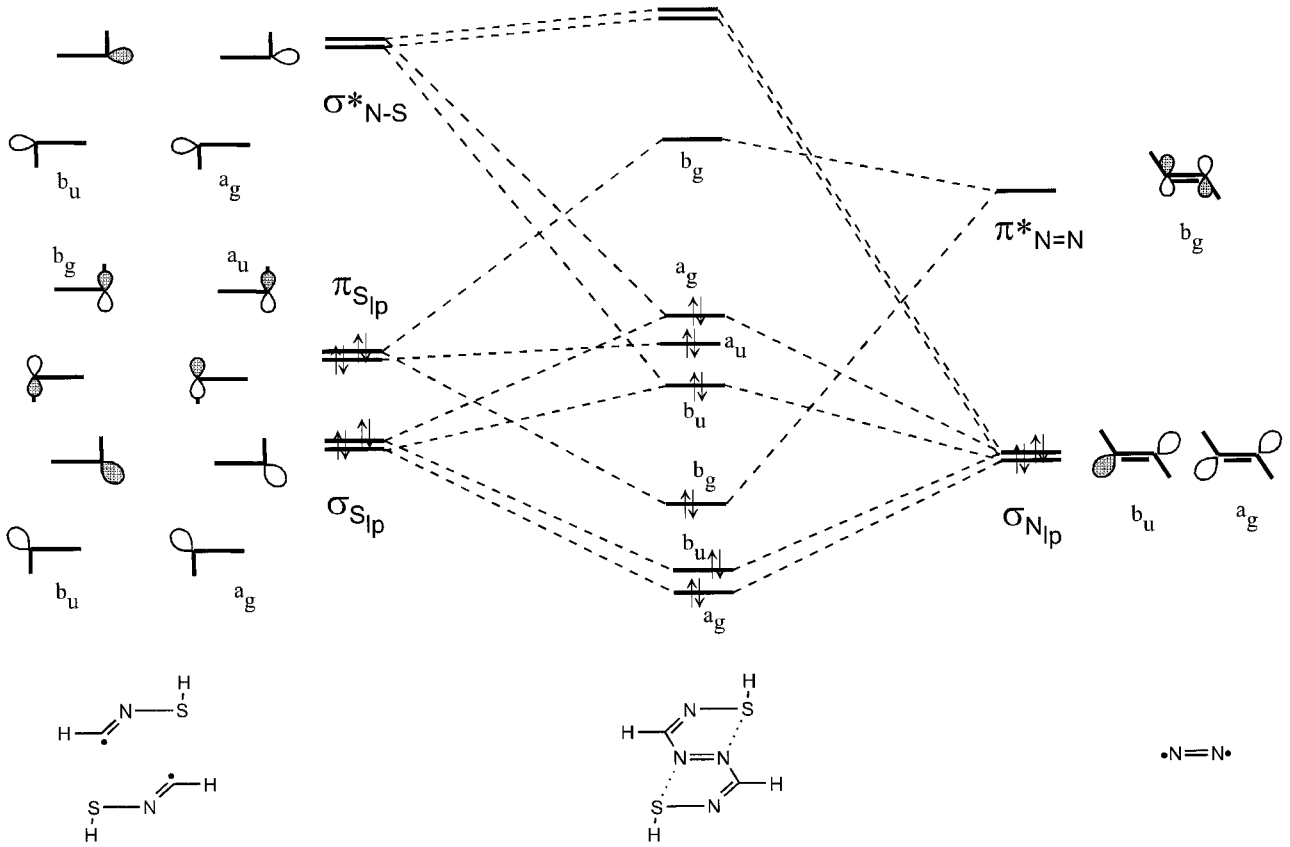

Figure 5. Orbital interactions for the fragments $(HEN{=}C(H)^{\bullet})_2$ and $^{\bullet}N{=}N^{\bullet}$.

isomers by intramolecular E···N interactions which are greatest for Te. In these and related chalcogen-containing diazenes such interactions involve back-donation from the chalcogen π lone pair into π^*(N═N) as well as donation from the σ(N) lone pairs into the σ^*(E−X) *and* σ^*(E−N) orbitals.

Note Added in Proof. The reaction of the *E,E,E* diazene **3b** with $Pt(PPh_3)_2(C_2H_4)$ produces the complex Pt[PhSNC(2-BrC_6H_4)N−N(2-BrC_6H_4)NSPh][PPh_3] in which the ligand is bonded to Pt in a tridentate S,N,N′ fashion analogous to that previously reported for the product of the reaction of the *Z,E,Z* diazene **1d** with $Pt(PPh_3)_2(C_2H_4)$.[45]

Acknowledgment. We thank the NSERC (Canada) for financial support. I.V.-B. acknowledges the award of a GraduateStudies scholarship from the DGAPA-UNAM (Mexico).

Supporting Information Available: Tables of experimental details for the crystal structure determinations of **1d** and **3b**, anisotropic thermal parameters, hydrogen atom coordinates and *U* values, bond lengths, bond angles, and torsion angles (12 pages). Ordering information is given on any current masthead page.

(45) Chivers, T.; McGregor, K.; Parvez, M. *Inorg. Chem.* **1994**, *33*, 2364.

IC960465J